Supporting information for:

Moderating the interaction among Pd, CeO_2, and Al_2O_3 for the improved three-way catalysts

Han Zhao [a,b,*], Longchun Bian [c], Junchen Du [a], Yunkun Zhao [a,*]

[a] *State Key Laboratory of Advanced Technologies for Comprehensive Utilization of Platinum Metals, Kunming Institute of Precious Metals, Kunming 650106, China*

[b] *Dalian Institute of Chemical Physics, Chinese Academy of Sciences, Dalian 116023, China*

[c] *School of Chemical Science and Technology, Yunnan University, Kunming 650091, China*

Email:

hanzhao@dicp.ac.cn (Dr. Han Zhao)

ykzhao@sohu.com (Prof. Yunkun Zhao)

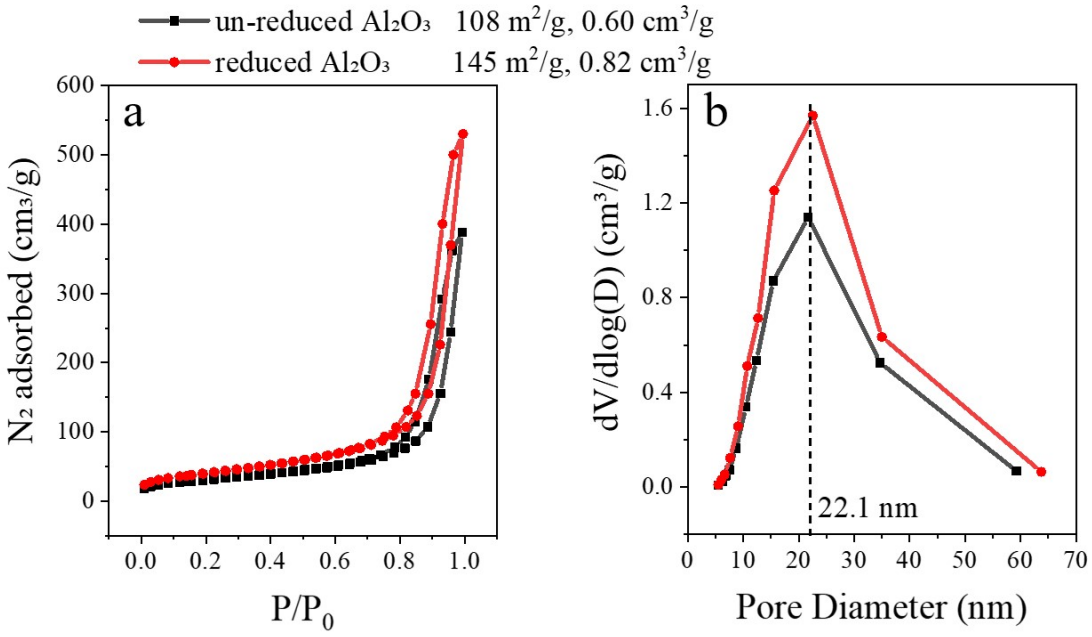

Fig. S1. The (a) isothermal N_2 adsorption/desorption curves and (b) the pore size distribution profiles of the different samples as indicated. The Al_2O_3 was reduced in 10% H_2/N_2 at 350 ℃ for 1h (ramp rate = 10 ℃/min), then was naturally cooled to room temperature (RT) in the tubular furnace

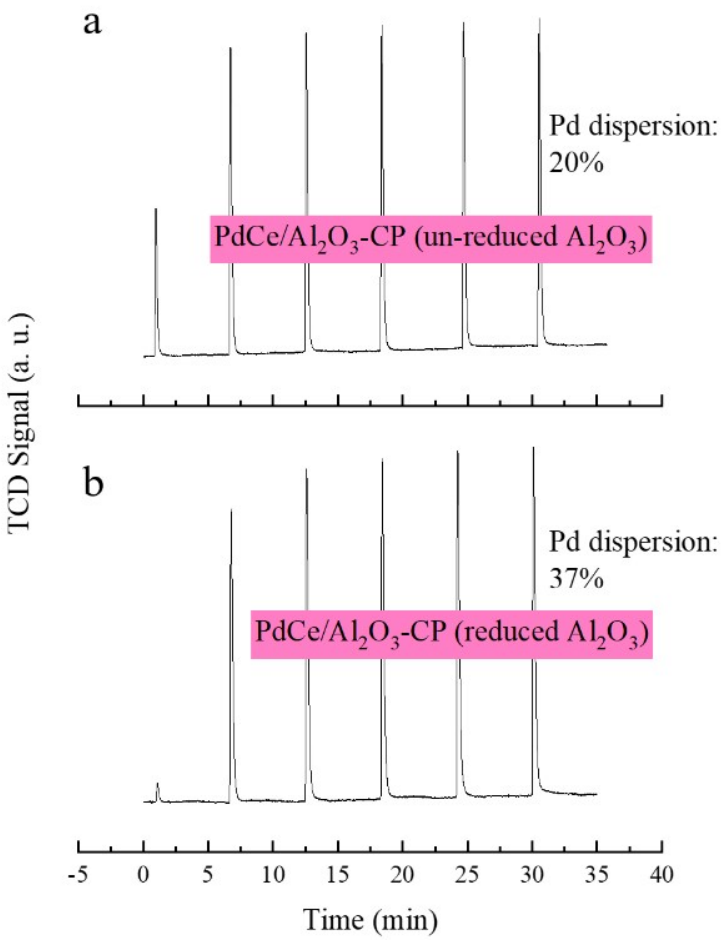

Fig. S2. The CO pulse-chemisorption curves of different catalysts as indicated. The PdCe/Al_2O_3-CP (reduced Al_2O_3) was identical to the PdCe/Al_2O_3-CP, and the PdCe/Al_2O_3-CP (un-reduced Al_2O_3) was made following the identical procedure to that of the PdCe/Al_2O_3-CP (reduced Al_2O_3) except that the un-reduced Al_2O_3 was adopted to replace the reduced Al_2O_3, hereinafter inclusive.

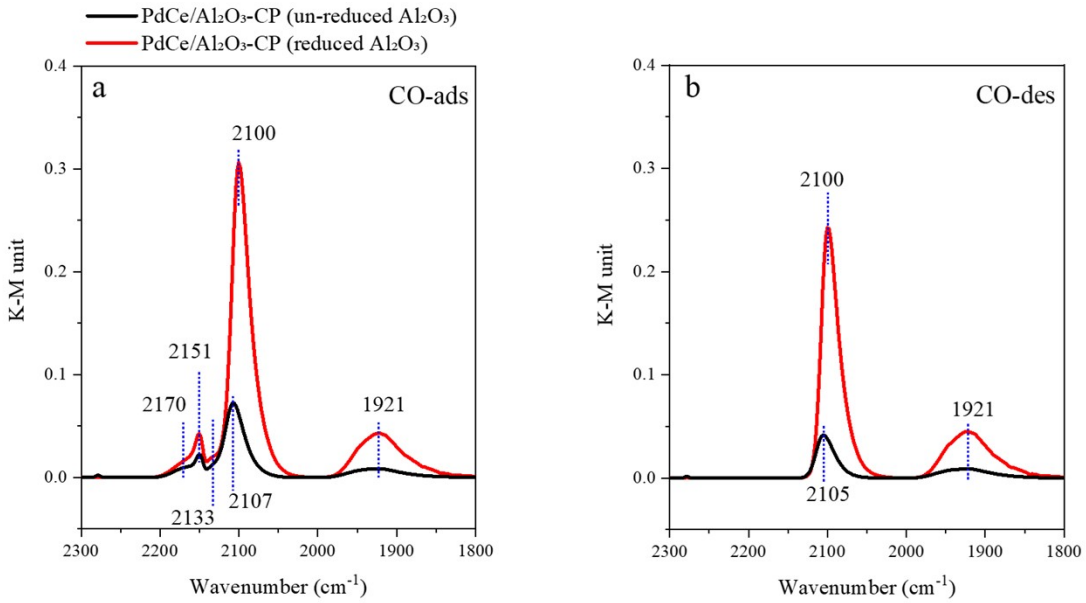

Fig. S3. The stabilized IR spectra of different catalysts during (a) CO adsorption in CO/He flow or (b) CO desorption in He flow.

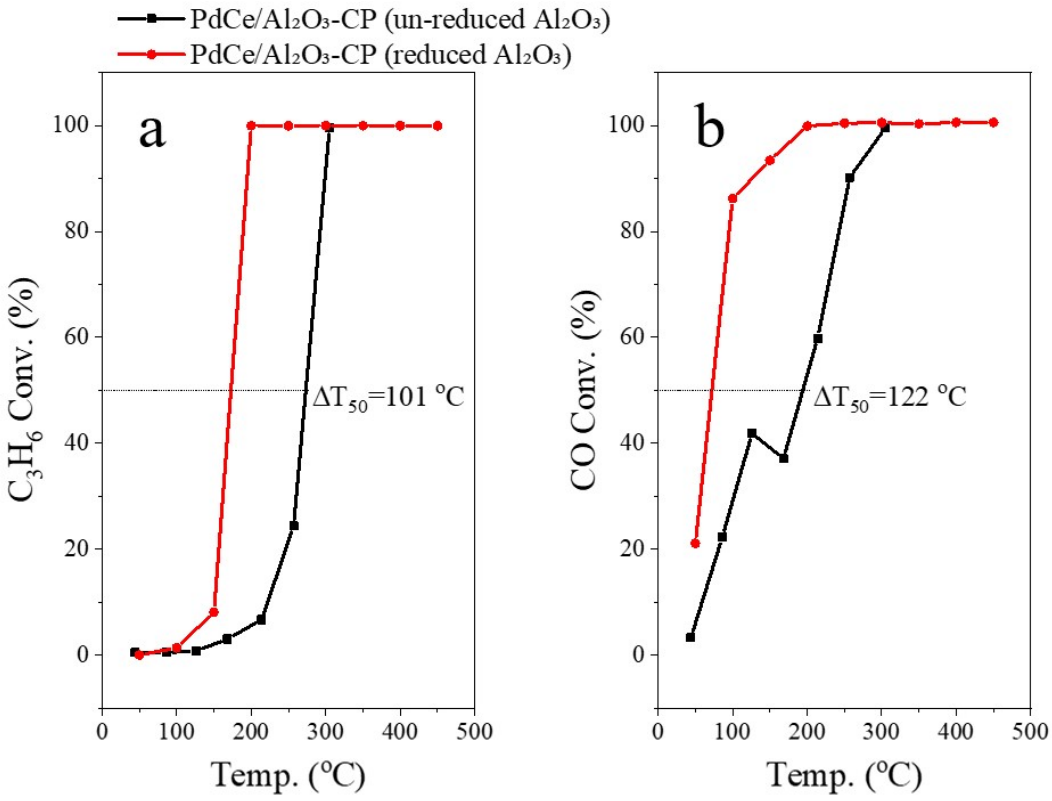

Fig. S4. Conversion-temperature curves of (a) C_3H_6 and (b) CO over the different catalysts as indicated.

Table S1. The structural properties of different samples.

	S_{BET} (m^2/g)	Pore Volume (cm^3/g)	Pore Size (nm)
Al_2O_3 (reduced)	145	0.82	22.1
$PdCe/Al_2O_3$-CP	120	0.58	17.4
$PdCe/Al_2O_3$-Imp	108	0.42	15.0

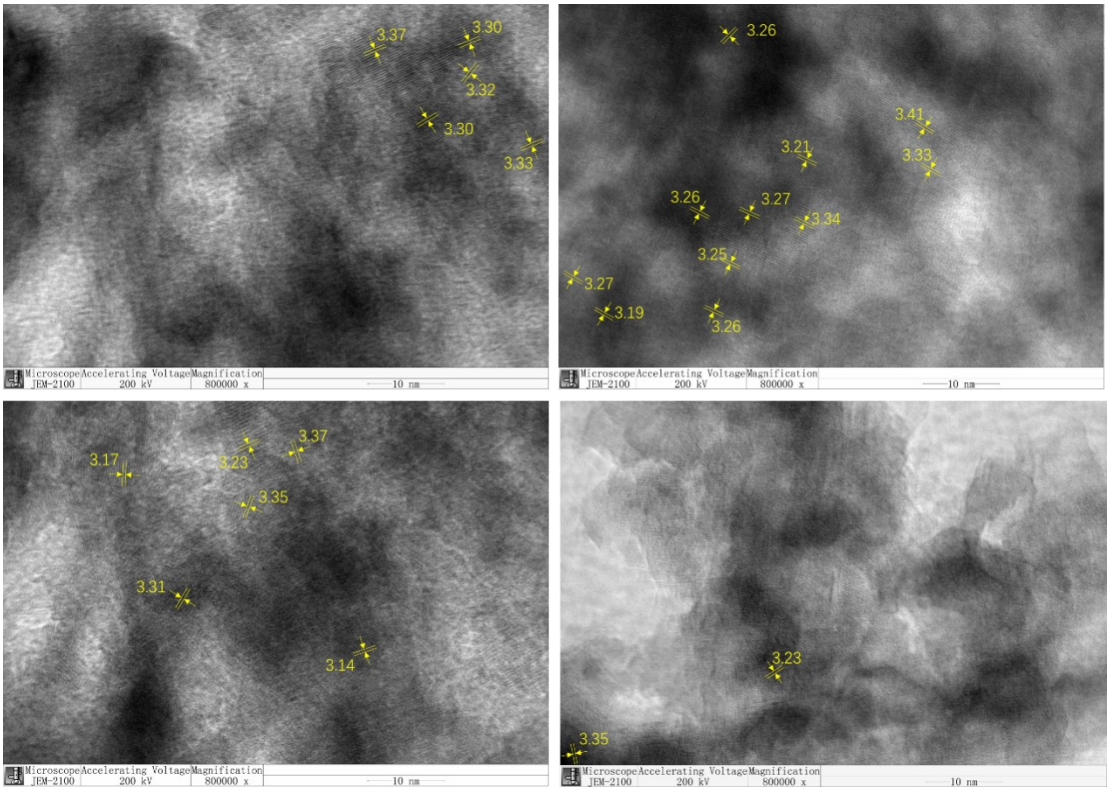

Fig. S5. HRTEM images of the $PdCe/Al_2O_3$-Imp. The lattice spacing of the CeO_2 facets were noted in Å.

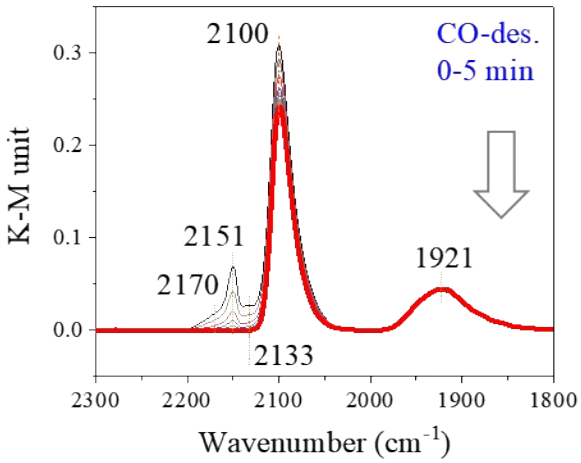

Fig. S6. The evolution of CO-DRIFTs curves over the PdCe/Al_2O_3-CP during CO desorption.

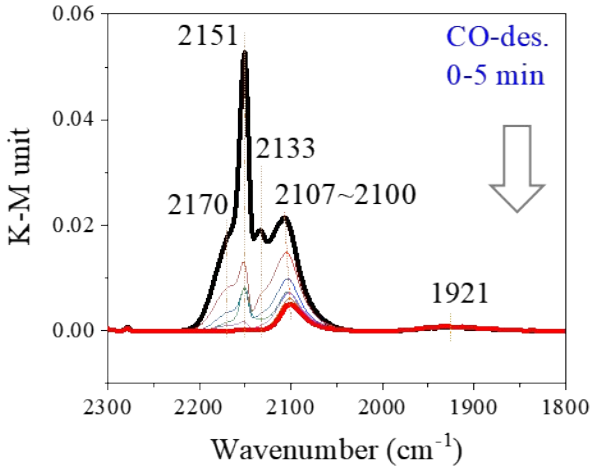

Fig. S7. The evolution of CO-DRIFTs curves over the PdCe/Al_2O_3-Imp during CO desorption.

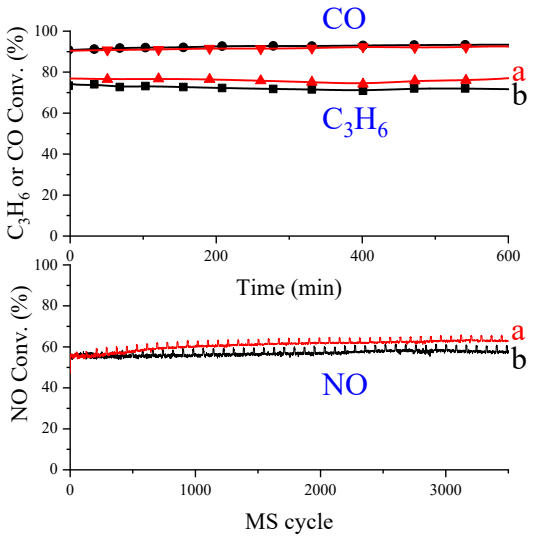

Fig. S8. The time-on-stream conversion of C_3H_6, CO, and NO over the different catalysts at 300 ℃ under an oxygen-deficient condition. a: PdCe/Al_2O_3-CP, b: PdCe/Al_2O_3-Imp. The concentrations of C_3H_6 and CO were measured by GC, while that of NO by MS. Conditions: 0.1 g of catalysts, 0.1% CO/ 0.1% C_3H_6/ 0.05% NO/ 0.166% O_2/ 8% CO_2/ 8 H_2O/ He, 150 mL/min.

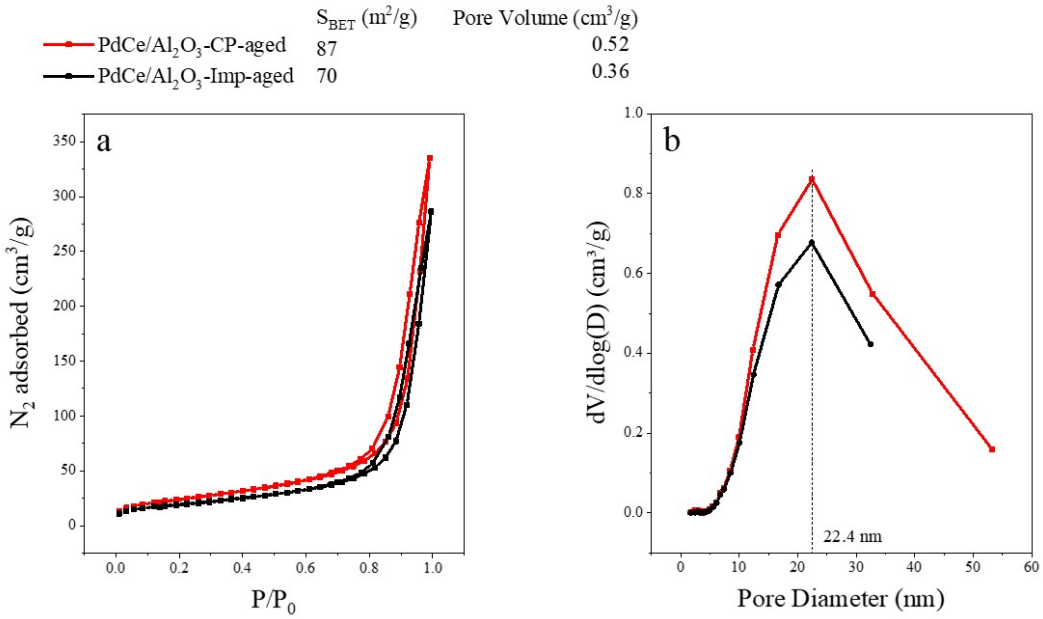

Fig. S9. The (a) isothermal N_2 adsorption/desorption curves and (b) the pore size distribution profiles of the different samples as indicated. the calcined PdCe/Al_2O_3-CP-c and PdCe/Al_2O_3-Imp-c samples were aged at 1000 ℃ in air for 4 h, then reduced by heating in 10% H_2/He from RT to 500 ℃, finally passivated in 1.5% O_2/N_2 at RT for 12 h to get the aged samples PdCe/Al_2O_3-CP-aged and PdCe/Al_2O_3-Imp-aged, respectively, hereinafter inclusive.

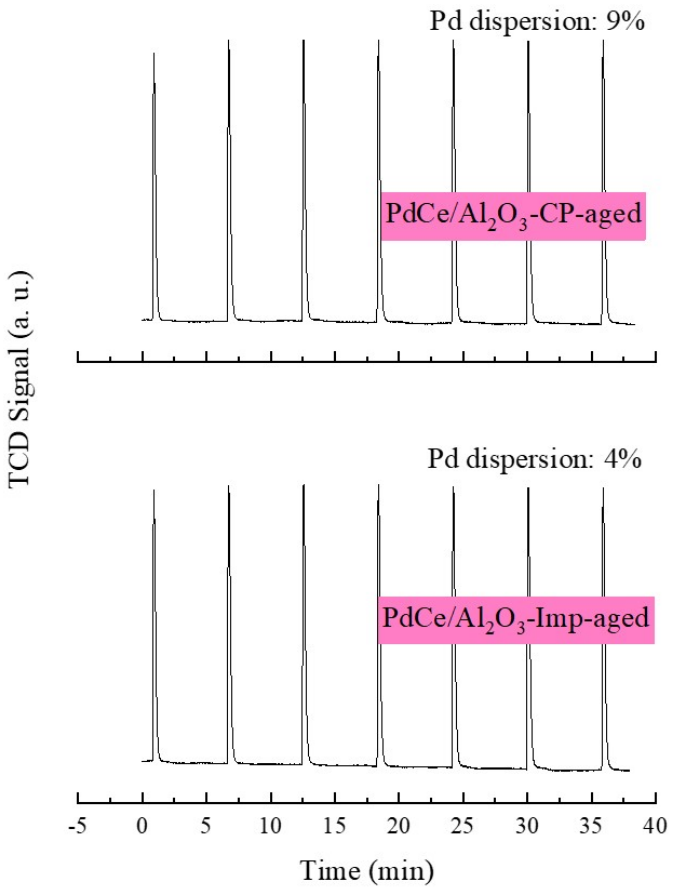

Fig. S10. The CO pulse-chemisorption curves of different catalysts as indicated.

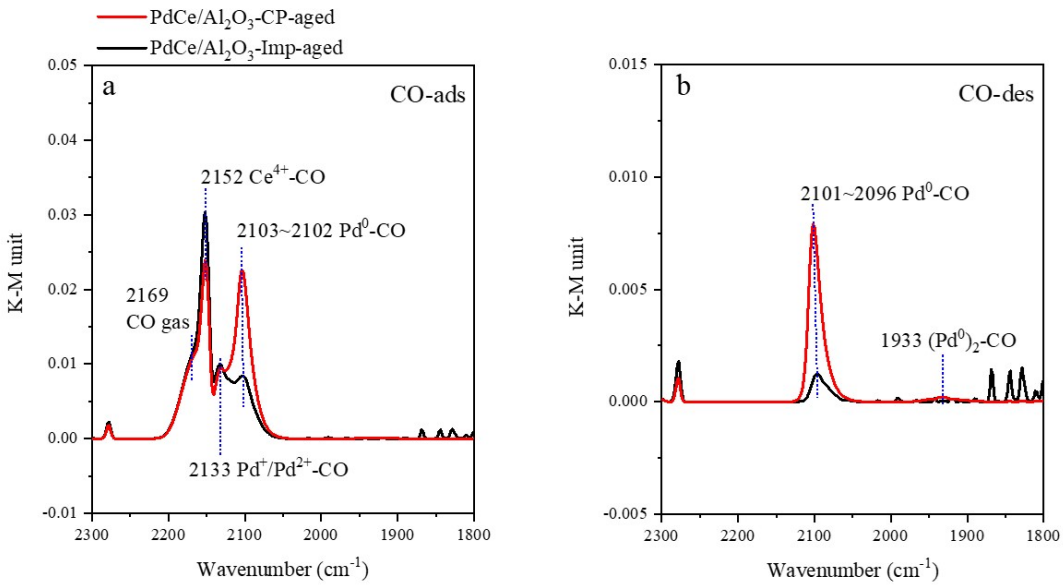

Fig. S11. The stabilized IR spectra of different catalysts during (a) CO adsorption in CO/He flow or (b) CO desorption in He flow.

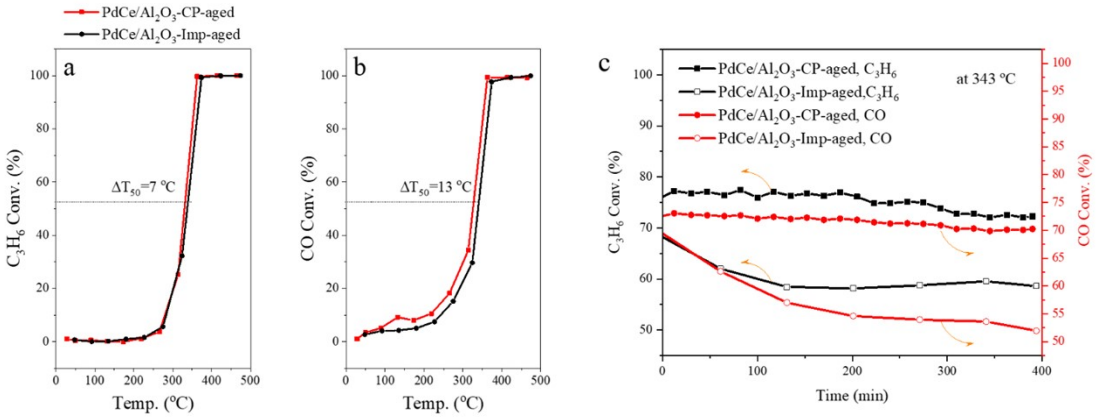

Fig. S12. Conversion-temperature curves of (a) C_3H_6 and (b) CO over the different catalysts as indicated. (c) Time-on-stream curves of the C_3H_6 and CO conversion over the different catalysts.

Table S2. The structural properties of different samples.

	S_{BET} (m^2/g)	Pore Volume (cm^3/g)	Pore Size (nm)	Pd dispersion
$PdCe/Al_2O_3$-CP	120	0.58	17.4	37
$PdCe/Al_2O_3$-Imp	108	0.42	15.0	15
$PdCe/Al_2O_3$-CP-aged	87	0.52	22.4	9
$PdCe/Al_2O_3$-Imp-aged	70	0.36	22.4	4